Journal of Power Sources 245 (2014) 236–244

Contents lists available at SciVerse ScienceDirect

Journal of Power Sources

journal homepage: www.elsevier.com/locate/jpowsour

Effect of the PTFE content in the gas diffusion layer on water transport in polymer electrolyte fuel cells (PEFCs)

Mehdi Mortazavi, Kazuya Tajiri*

Mechanical Engineering – Engineering Mechanics, Michigan Technological University, 1400 Townsend Drive, Houghton, MI 49931, USA

HIGHLIGHTS

- Taking an *ex-situ* approach, water droplet behavior on gas diffusion layer (GDL) surface was studied.
- Impacts of PTFE content in GDL, gas velocity, and gas species were studied.
- Gas velocity was observed to have a significant effect on droplet detachment diameter.
- Droplet contact angles were observed to be similar on GDLs with different amount of PTFE.

ARTICLE INFO

Article history:
Received 9 April 2013
Received in revised form
18 June 2013
Accepted 19 June 2013
Available online 2 July 2013

Keywords:
Water management in PEFC
Gas diffusion layer
Droplet detachment diameter
Contact angle
Surface adhesion force
Drag force

ABSTRACT

The dynamic behavior of a liquid water droplet emerging and detaching from the surface of the gas diffusion layer (GDL) is investigated. The droplet growth and detachment are studied for different polytetrafluoroethylene (PTFE) contents within the GDL and for different superficial gas velocities flowing in the gas channel. To simulate the droplet behavior in the cathode and anode of an operating polymer electrolyte fuel cell, separate experiments are conducted with air and hydrogen being supplied in the gas channel, respectively. Both the superficial gas velocity and the PTFE content within the GDL are found to impact the droplet detachment diameter. Increasing the superficial gas velocity increases the drag force applied on the droplet sitting on the GDL surface. It is observed that the droplet detaches at a smaller diameter for higher superficial gas velocities. The droplets also detach at smaller diameters from GDLs with a higher amount of PTFE. Such observation is justified according to two different points of view: (1) heterogeneous through-plane PTFE distribution through the GDL and (2) reduced GDL surface roughness caused by PTFE loading.

1. Introduction

Polymer electrolyte fuel cells (PEFCs) are considered to be promising power sources for automotive, residential and stationary applications [1]. They benefit from high efficiency as well as a high volumetric power density without emitting greenhouse gases as they operate. However, there are some issues that need to be solved before this type of energy system can be commercially released. One of the most challenging issues for researchers is water management in PEFCs. As electrochemical reactions occur in PEFC, hydrogen fuel is converted into useful power with water and heat as byproducts. Some portion of this produced water may be helpful in increasing the cell performance by hydrating the membrane and improving its proton conductivity. Some other portion of the water produced in the cathode may be transported into the anode by back diffusion or evaporate into the gas channel. Any excess amount of liquid water fills open pores in the gas diffusion layer (GDL). Increasing the amount of liquid water within the GDL can ultimately saturate the GDL. This will block the transport of reactants to the catalyst layer. This phenomenon is known as flooding and is reported to significantly decrease the performance of the cell [2–4]. Flooding mostly happens at high current densities when the water production rate is considerable. It may also occur at low current densities under certain conditions such as low temperature and low reactant flow rates. The accumulated liquid water within the GDL emerges from the GDL surface in the form of droplets. Liquid water removal from the GDL surface follows two different modes depending on the water production rate as well as the superficial gas velocity [5]. The superficial gas velocity is defined as the bulk velocity of gas flowing within the channel cross sectional area. For a high superficial gas velocity, the shear force from the core gas flow causes the droplets to detach from the GDL surface. When the superficial gas velocity is

* Corresponding author.
E-mail addresses: mortazav@mtu.edu (M. Mortazavi), ktajiri@mtu.edu (K. Tajiri).

0378-7753/$ – see front matter © 2013 Elsevier B.V. All rights reserved.
http://dx.doi.org/10.1016/j.jpowsour.2013.06.138

moderate, the droplets grow in size until they touch the hydrophilic channel walls and spread over them. In this case, the capillary flow drains the liquid water through the corners and forms an annular film flow. When the water production rate is high and/or the superficial gas velocity is low, the corner flow is not capable of draining all of the liquid water from the gas channel. In this case, the liquid film grows in size and ultimately clogs the gas channel. This eventually stops the cell from producing electricity.

It is a common practice to treat GDLs with a hydrophobic agent such as polytetrafluoroethylene (PTFE) for better liquid water transport within the GDL [6]. Many works have targeted the effect of GDL treatment on the cell performance [7–12] as well as its effect on the liquid water behavior within the cell [13–15]. Although all these works agree on improved cell performance with the addition of some amount of PTFE to the raw GDL, a common conclusion about the role of PTFE in the GDL on liquid water transport has not been reached. Some works suggest that increasing the PTFE content in the GDL lowers the liquid water transport rate through the GDL [8,16]. Some other works confirm that a GDL with a slight amount of PTFE content shows significantly lower water wetting compared to an untreated GDL but that adding more PTFE does not affect water wetting on the GDL surface [17,18]. Although applying PTFE in the GDL mainly affects the water behavior within the cell, its impacts on other parameters should also be considered for an appropriate cell design. It has been found that increasing the PTFE content within the GDL has some drawbacks such as decreased electrical conductivity [12,19], thermal conductivity [20], permeability [8,12] and porosity [12,21,22].

Within the last few decades, different experimental approaches have been taken to study the liquid water transport and distribution in PEFCs. Methods such as neutron imaging [23,24], gas chromatography (GC) [25,26] and X-ray techniques [27,28] have enabled the *in-situ* observation of the liquid water distribution within PEFC. The application of these *in-situ* observation methods is complex and expensive. Furthermore, these methods are either limited in spatial and temporal resolution (neutron radiography) or not applicable to situations with an abundant amount of liquid water (GC). Direct optical visualization, on the other hand, is most likely the simplest and the least expensive method to monitor liquid water behavior in PEFC. Depending on the optical setup used, it can also benefit from high spatial and temporal resolution.

Although many studies on direct optical visualization have been conducted [4,5,13,15,29,30], there have been very few published reports studying droplet growth and detachment on the GDL surface with different wettabilities.

Theodorakakos et al. [31] made a direct visualization experimental setup and recorded the droplet's side view behavior upon detachment. They measured the dynamic contact angle of the droplet and could correlate the droplet detachment diameter with the air velocity. It was found that for any given droplet size, there is a critical value of superficial gas velocity above which the droplet can be detached from the surface of the GDL. Bazylak et al. [32] studied droplet growth and detachment from the GDL surface by using fluorescence microscopy and observed that the breakthrough location changes over time. This observation was followed by modeling the GDL as an interconnected network of water pathways. The other observation reported in the same study [32] was the layer of residual water that detaching droplets leave on the GDL surface. This layer was considered to provide the pinning site for prospective droplets emerging from the GDL surface. Although this work was successful in defining the dynamic behavior of liquid water transport through the GDL, the influence of the surface energy on droplet behavior was not studied.

Kumbur et al. [29] used direct visualization and measured the contact angle hysteresis (the difference between the advancing and receding contact angles) as a parameter that determines the instability of the droplet under the influence of a shear gas flow. It was observed that the contact angle hysteresis increased with the PTFE content for any given superficial air velocity. Consequently, a droplet placed on the GDL surface of a high PTFE content tended to be more unstable and could be removed more easily. Very recently, Das et al. [33] studied droplet detachment from the GDL surface by measuring the sliding angle and noticed that liquid columns formed underneath the droplet and within the GDL pores, which assisted the droplet's adhesion to the GDL surface.

The illustrated literature review highlights the lack of in-depth studies of the droplet behavior on the GDL surface with different PTFE contents. In this work, the droplet growth and detachment from GDLs with different PTFE contents and under different superficial gas velocities are quantitatively studied. A scaled-up channel is designed to eliminate the wall effect. Although channel walls may affect the droplet growth and detachment mechanism, the droplet behavior under the influence of a core gas flow is the subject of study in this work.

2. Experimental setup

2.1. Apparatus design

An *ex-situ* direct visualization apparatus was designed and fabricated to study liquid water droplet emergence, growth and detachment on the GDL surface, as shown in Fig. 1. The experimental apparatus includes a 100 mm long, 2.5 mm wide single gas channel machined on a 1 mm thick aluminum plate and sandwiched between two polycarbonate plates. Air or hydrogen was supplied within the gas channel through an inlet port machined on one of the polycarbonate plates. The inlet port was aligned with the gas channel at its entrance. The GDL sample was placed between polycarbonate plate 1 and the aluminum plate (Fig. 1). Deionized liquid water was injected by a syringe pump on one side of the GDL (the side facing polycarbonate plate 1) through a capillary tube with an inside diameter of 250 μm (U_111, Upchurch). The droplet emergence, growth, and detachment on the other surface of the GDL were monitored through polycarbonate plate 2. Teflon sheets were used between the polycarbonate plates and the aluminum plate to prevent any possible gas leakage from the apparatus.

Toray carbon papers (TGP_060) with a manufacturer-specified thickness and porosity of 190 μm and 76%, respectively, were used as the GDL. Toray carbon papers were loaded with PTFE based on the procedure presented in Ref. [34]. This procedure is described as follows. The substrates were dipped in PTFE emulsion (60 wt.% dispersion in H_2O, ALDRICH) for 10 h, and then they were dried at 120 °C for 1 h. According to Ref. [34], to make a uniform distribution of PTFE within the GDL substrates, the substrates were sintered at 360 °C for 1 h. The PTFE weight percent loaded on the GDL was controlled by the PTFE concentration in the emulsion.

To study the aging effect on the GDL surface energy, the GDL samples were aged in two steps. In the first step, the GDL samples were dipped in deionized water at 60 °C for 24 h. For the second

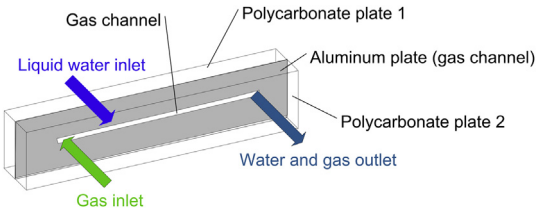

Fig. 1. Experimental apparatus.

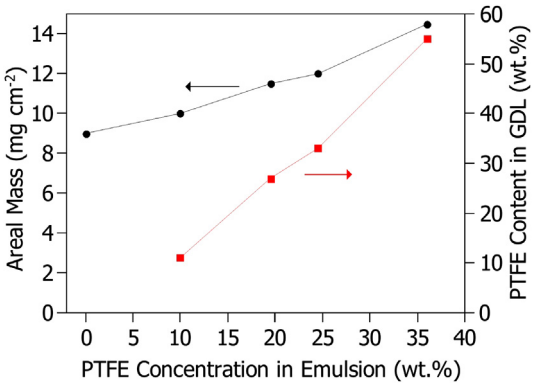

Fig. 2. GDL areal mass and PTFE content based on PTFE concentration in emulsion.

step, the GDL samples were removed from the deionized water and put in the furnace at 60 °C for 4 h.

Fig. 2 shows the amount of PTFE content in the GDL as well as the loaded GDL areal mass based on the PTFE concentration in the emulsion. The PTFE content in the GDL was calculated by comparing the GDL mass before and after the PTFE treatment. Samples with nominal PTFE loadings of 10 wt.%, 25 wt.%, 35 wt.% and 55 wt.% were tested in this study. Table 1 summarizes the measured and calculated physical properties of the samples.

For a better clarification of the droplet behavior on the GDL surface in the cathode and anode of an actual fuel cell, separate experiments were conducted with air and hydrogen being supplied in the channel, respectively. Two different range rotameters (Omega, FL_3802C and FL_3804ST) were used to supply the desired volumetric gas flow rate at low (max. 1200 ml min^{-1} for air and 4200 ml min^{-1} for hydrogen) and high (max. 4500 ml min^{-1} for air and 16,000 ml min^{-1} for hydrogen) ranges. All experiments were run in atmospheric pressure and at room temperature. The GDL surface temperature was measured as 59 °C ± 1 °C using a hand-held infrared thermometer (Optex). This relatively high temperature came from two light sources used during the experiments. Table 2 lists the conditions of each run in the series of experiments. Three runs were conducted for each case to ensure repeatability. To provide the same condition for each run, the GDLs were dried by purging nitrogen at 3000 ml min^{-1} for 20 min while the two light sources were kept on. The schematic of the experimental setup consisting of the experimental apparatus, gas cylinder, rotameter, syringe pump and high speed camera controlled by a PC is shown in Fig. 3.

2.2. High speed imaging

The droplet growth and detachment on the GDL surface in the gas channel was recorded using a high speed camera (50KD2B2, Mega Speed) controlled with a PC. A Navitron TV Zoom Lens 7000 18_180 mm was attached to the high speed camera that provided a spatial resolution of 10 μm $pixel^{-1}$. The visualizing window had a resolution of 640 × 480 pixels with approximately 250 pixels for the channel width. This ensured a proper resolution for image analysis. Image analysis was performed by the Mega Speed AVI Player software provided by the camera manufacturer. Two 300-W tungsten lamps (Lowel Omni) were used as the light source to provide proper illumination.

Table 1
GDL properties for different PTFE loading.

Nominal Teflon loading	Static contact angle measured (fresh)	Static contact angle measured (aged)	Areal mass mg cm^{-2}	Calculated Teflon loading
0 wt.%	129.7° ± 8.84°	NA	9 ± 0.2	NA
10 wt.%	153.7° ± 1.57°	147.3° ± 1.49°	10 ± 0.3	11 wt.%
25 wt.%	152.8° ± 3.1°	148° ± 3.27°	11.5 ± 0.3	27 wt.%
35 wt.%	151.7° ± 3°	147.3° ± 3.27°	12 ± 0.5	33 wt.%
55 wt.%	153.5° ± 1.7°	146.9° ± 2.49°	14.5 ± 0.7	55 wt.%

2.3. Contact angle measurement

The static contact angles on fresh and aged GDLs were measured using a setup already made for this purpose [35]. The procedure and theory can be found in Ref. [36]. The contact angle measurement setup consisted of an illumination source that provided a beam of light with equal intensity, a series of lenses to converge the beam, a labjack (Thorlabs L200) enabling X_Y_Z alignment of the sample and a long distance microscope (Infinity K2/S) coupled to a CCD camera (PULNIX TM-1325CL). Ten droplets with diameters in the range of 1–3 mm were placed on the GDL surfaces, and images were captured. The images were then analyzed with a computer code developed based on the Young–Laplace equation. The mean value of the contact angle for the ten images was considered the contact angle of the droplets on each GDL surface.

2.4. Flow condition

The surface area of the capillary tube, (4.908×10^{-4} cm^2), used to inject liquid water on the GDL surface can be considered the water production area in an operating fuel cell. The water production rate during the oxygen reduction reaction can be obtained by Faraday's second law of electrolysis:

$$\dot{n}_{H_2O} = \frac{iA_{act}}{2F} \quad (1)$$

where $\dot{n}_{H_2O}$ is the molar rate of water produced, i is the current density, A_{act} is the active area, and F is Faraday's constant. Assuming all water produced is in the liquid phase, the liquid water production rate for a current density of 2 A cm^{-2} and an active area of 4.908×10^{-4} cm^2 is 0.33 μl h^{-1}. To be able to run the experiment in a reasonable amount of time and without secondary effects such as evaporation, a water flow rate of 350 μl h^{-1} was chosen, as in Ref. [37].

Air and hydrogen were supplied at different ranges, as given in Table 2. These flows result in Reynolds numbers ranging from 336 to 1345 for air and from 252 to 672 for hydrogen.

3. Results and discussion

3.1. Contact angle

The liquid contact angle is a measure of the wetting ability of a solid surface by liquid and depends on the interfacial energy along the three phase boundary. In water management with application in PEFC, the contact angle is an important parameter characterizing many dominant properties. The surface adhesion force, drag force, capillary pressure, and even the shape of a droplet sitting on the GDL surface are some of the properties that the contact angle affects. The surface adhesion force, which is the consequence of the molecular interaction between a liquid and a solid, makes the droplet adhere to the solid surface. This force holds the droplet on the GDL surface by resisting the drag force from the core gas flow. It has been shown that the contact angle hysteresis is a key parameter in defining the adhesion force and instability of a droplet under the influence of a shear gas flow [29,38]. Increasing the gas flow rate

Table 2
Experiment conditions.

Run	Nominal PTFE wt.%	Gas	Flow rate ml min^{-1}	Superficial gas velocity m s^{-1}	Reynolds number	Water injection rate μl h^{-1}	Video frame rate (fps)
A1	0	Air	1666	11.1	1009	350	200
A2	10	Air	1666	11.1	1009	350	200
A3	25	Air	1666	11.1	1009	350	200
A4	35	Air	1666	11.1	1009	350	200
A5	55	Air	1666	11.1	1009	350	200
A6	0	Air	2222	14.8	1345	350	50
A7	25	Air	555	3.7	336	350	200
A8	25	Air	1111	7.4	672	350	200
A9	25	Air	2222	14.8	1345	350	100, 150, 200
H1	10	Hydrogen	6000	40	504	350	150
H2	25	Hydrogen	6000	40	504	350	150
H3	35	Hydrogen	6000	40	504	350	150
H4	55	Hydrogen	6000	40	504	350	150
H5	25	Hydrogen	3000	20	252	350	150
H6	25	Hydrogen	4000	26.6	335	350	150
H7	25	Hydrogen	5000	33.3	419	350	150
H8	25	Hydrogen	7000	46.6	587	350	150
H9	25	Hydrogen	8000	53.5	672	350	150
H10	35	Hydrogen	3000	20	252	350	150
H11	35	Hydrogen	4000	26.6	335	350	150
H12	35	Hydrogen	5000	33.3	419	350	150
H13	35	Hydrogen	7000	46.6	587	350	150
H14	35	Hydrogen	8000	53.5	672	350	150

increases the dynamic contact angle hysteresis and moves the droplet toward an unstable condition [29]. The contact angle of a droplet on a PTFE-treated GDL depends on parameters such as the porosity, macroscopic roughness of fibers ridges, microscopic roughness of the individual fibers, and chemical heterogeneity of the carbon and PTFE surface in the GDL [18]. In this study, the static contact angle was measured and used as the parameter defining the surface energy of GDLs.

Sessile droplets on treated and untreated GDLs are shown in Fig. 4. The GDLs were aged by dipping them in deionized water at 60 °C for 24 h and then drying them in a furnace at 60 °C for 4 h Fig. 5 shows the contact angles of the droplets on fresh treated, aged treated, and fresh untreated GDLs. The error bars shown represent the standard deviation of the measured contact angles. While adding some amount of PTFE to an untreated GDL significantly increases the contact angle, it can be observed that the droplets show similar contact angles on GDLs with different PTFE contents. A similar observation was reported by Benziger et al. [39] for TGP-H-120 Toray carbon paper. Lim and Wang [9] calculated the contact angle based on a capillary meniscus height measurement and observed that the contact angle does not change significantly by adding Teflon from 10 wt.% to 40 wt.% PTFE. Fairweather et al. [17] used the pore size distribution obtained from MIP to estimate the effective contact angle distributions on untreated and treated GDLs. It was observed that the contact angle increases by applying 5 wt.% PTFE to a raw GDL and that any further addition of PTFE does not have any effect on the contact angle. Because the contact angle does not change with the PTFE content in the GDL, it is suspected that most of the PTFE particles penetrate through the GDL and agglomerate within the pores rather than on the GDL surface. Furthermore, the comparable contact angles of treated fresh GDLs (152°) and treated aged GDLs (147°) support the possibility of higher PTFE agglomeration within the GDL rather than on its surface. However, there should be some PTFE particles sitting on the surface of the GDL because the contact angle is significantly different between an untreated GDL and a 10 wt.% PTFE-treated GDL. PTFE particles are small enough (50–500 nm) to be able to pass through GDL pores (10–30 μm) and accumulate on the inner layers of the GDL. The smaller standard deviations of the contact angles on the treated GDLs shown in Fig. 5 represent more uniform contact angles on treated GDLs compared to untreated ones. The PTFE particles fill the open pores on the GDL surface and make a smooth surface with a shorter contact line between the droplet and fibers.

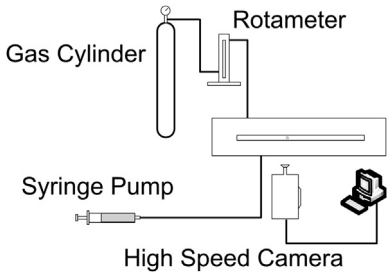

Fig. 3. Schematic of experimental setup.

3.2. Droplet growth

Liquid water finds the path with the least transport resistance through the GDL and emerges from preferential locations, forming droplets [40]. The emerged droplet grows in size until it becomes large enough to detach from the GDL surface. However, a low superficial gas velocity is not capable of detaching the droplet. Fig. 6 shows the droplet growth on untreated and treated GDLs with different PTFE contents. The spreading factor, defined as the ratio of the droplet diameter d to the droplet detachment diameter d_d, is shown at different times. The spreading factor is only shown for the first 100 ms for the sake of comparison. Fig. 6 shows that as the PTFE content in the GDL increases, the slope of the spreading factor curve increases. This means that for GDLs with a higher amount of PTFE droplets needs less time to reach the size at which they detach. Fig. 6 also shows that for 35 wt.% and 55 wt.% PTFE, detachment occurs within 100 ms, while a longer time is required for droplets to detach from GDLs with a lower amount of PTFE.

3.3. Droplet detachment diameter

Zhang et al. [5] defined two modes of water removal from a GDL surface, droplet detachment by shear force and capillary wicking of

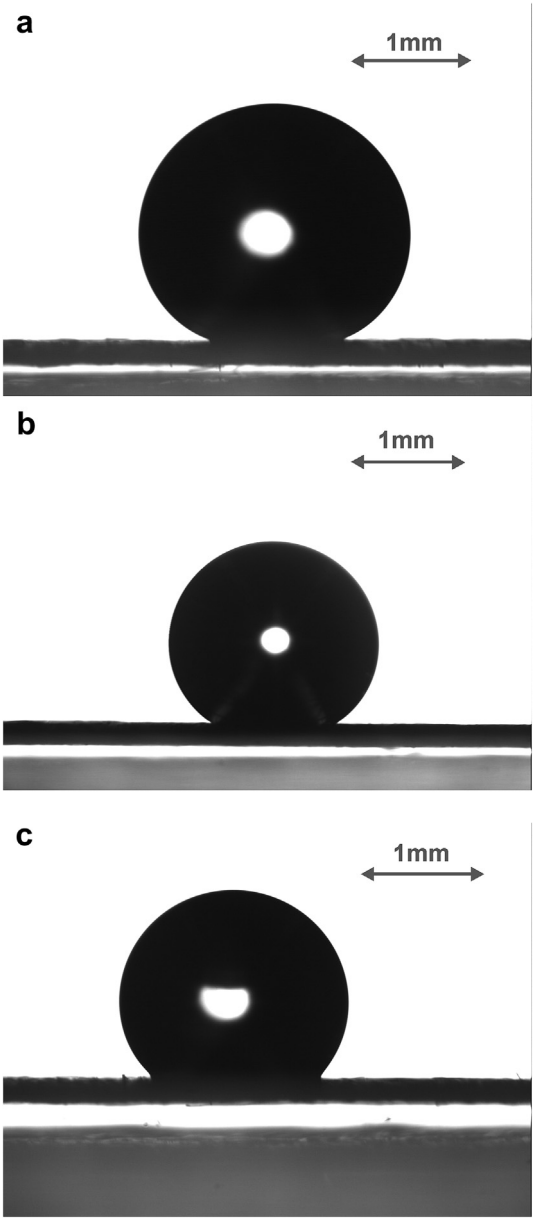

Fig. 4. Contact angle measurement (a) 10 wt.% PTFE treated fresh GDL, contact angle = 153.7° ± 1.57°, (b) 10 wt.% PTFE treated aged GDL, contact angle = 147.3° ± 1.49°, (c) untreated fresh GDL, contact angle = 129.7° ± 8.84°.

liquid water into more hydrophilic channel walls. Droplet detachment is the characteristic of a high superficial gas velocity, while capillary wicking occurs at lower gas flow rates. The droplet detachment from GDLs with different wettabilities is the subject of study in the present work. Droplet detachment can be studied by considering all of the forces applied on a droplet under a shear gas flow. Considering the droplet free body diagram as shown in Fig. 7, these forces are (i) the gravitational force (F_G), (ii) the surface adhesion force (F_S) and (iii) the shear drag force from core gas flow (F_D).

The Bond number describes the ratio of the gravitational force to the surface tension force and is defined as:

$$\mathrm{Bo} = \frac{\Delta\rho g d_d^2}{\sigma} \tag{2}$$

where $\Delta\rho$ is the density difference between the liquid and the gas, g is the gravitational acceleration, d_d is the droplet detachment diameter and σ the interfacial surface tension. The maximum Bond number calculated in this study was 0.1, which indicates that the force of gravity is small compared to the surface tension and can be neglected [41]. The surface adhesion force keeps the droplet on the surface, while the drag force applied from the core gas flow tries to detach the droplet from the surface. Droplet detachment occurs when the drag force overcomes the surface adhesion force.

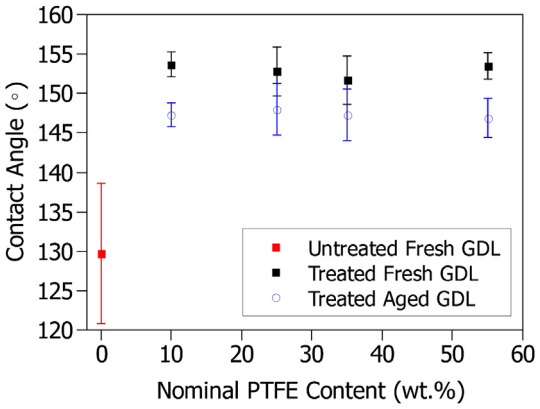

Fig. 5. Droplet contact angle on treated and untreated GDLs.

The droplet detachment diameter is an important parameter in fuel cell gas channel design. A gas channel smaller than the droplet size will be clogged by the droplet upon detachment. An over-sized channel, on the other hand, will increase the parasitic power required to supply the reactants at the same superficial velocity to run the cell. The former stops the cell from producing energy, and the latter lowers the overall energy efficiency.

Comparing the hydrogen and air superficial velocities upon droplet detachment shows that a higher hydrogen velocity is required to detach a droplet from the GDL surface. This behavior can be justified by hydrogen's lower density compared to air. The drag force is a function of the gas velocity and the gas density. Because hydrogen density is lower than air density, a higher superficial hydrogen velocity will be required to provide enough drag force to detach a droplet. The drag force applied from a core gas flow on a droplet can be calculated by:

$$F_D = \frac{1}{2}\rho C_D A_P V^2 \tag{3}$$

where ρ is the gas density, C_D is the drag coefficient, A_P is the projected area, and V is the superficial gas velocity.

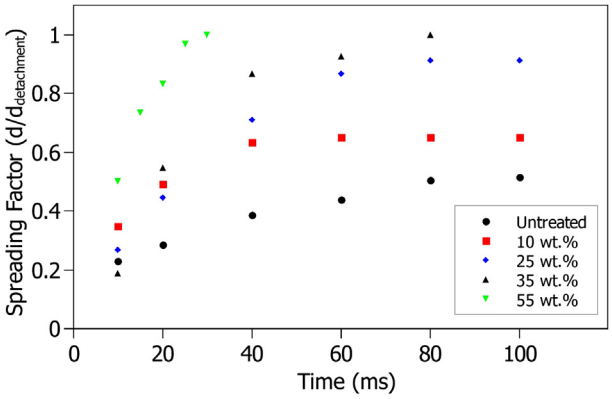

Fig. 6. Droplet growth rate under superficial air velocity of 11.1 m s^{-1} on treated and untreated GDLs.

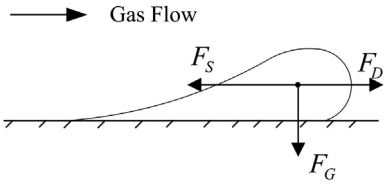

Fig. 7. Forces applied on a droplet in general configuration.

It was also observed that droplets leave residual liquid water particles as they detach from the GDL surface. It has been reported that these residual water particles become the pinning site for future droplets and are followed by slug formation after a while [32].

The location of the droplet's emergence was also studied in this work. It was observed that the first few droplets emerged and detached at a constant location. However, prospective droplets showed a tendency to appear from different locations, as shown in Fig. 8. This suggests an interconnected network of water pathways within the GDL, as was reported by Bazylak et al. [32].

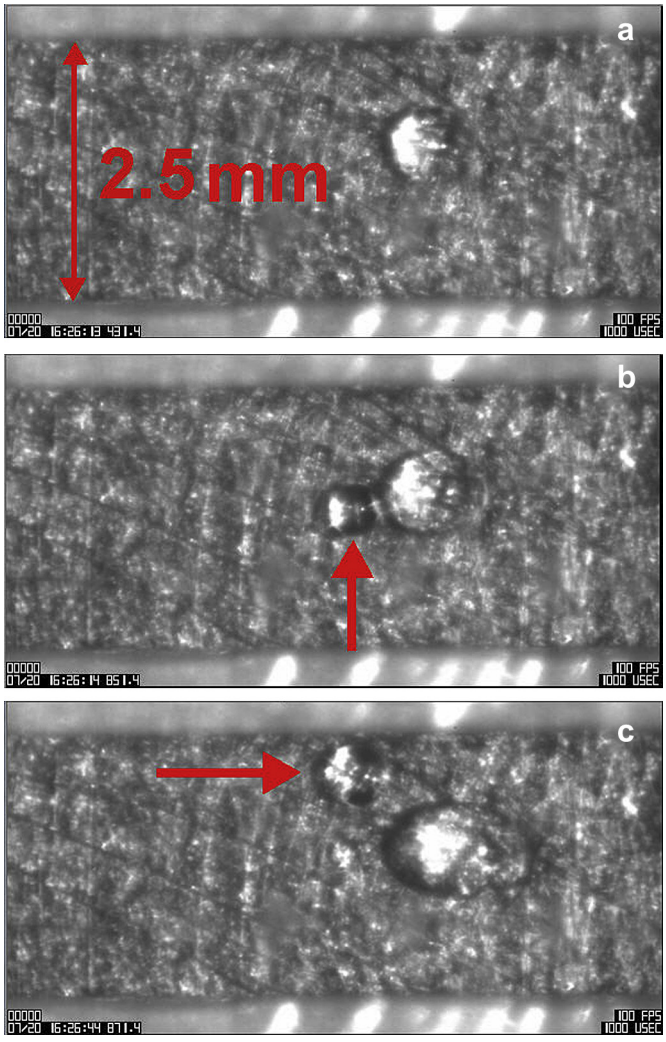

Fig. 8. Multiple droplets emerging at different breakthrough locations on 10 wt.% PTFE GDL surface; (a) breakthrough location for first few droplets, (b, c) droplets emerging at different locations after a while.

3.3.1. Effects of the PTFE content on the droplet detachment diameter in the cathode and anode

Fig. 9 shows the droplet detachment diameter on GDLs with different PTFE contents and under a superficial air velocity of 11.1 m s^{-1}. Each data point represents the mean diameter of the first ten detaching droplets for three separate runs. As the figure shows, the droplet detachment diameter decreases as the PTFE content within the GDL increases. As shown in Fig. 5, the droplet contact angles on the PTFE-treated GDLs are almost uniform and do not change with the PTFE content. The fact that the PTFE content within the GDL affects the droplet detachment diameter without having any contribution to the droplet surface contact angle can be an indication of the existence of a heterogeneous through-plane parameter affecting the liquid water transport within the GDL.

A smaller detachment diameter on GDLs with a higher PTFE content can be justified by PTFE accumulation within the GDL. It has been reported that the PTFE distribution through the GDL is not uniform and varies through the GDL thickness. Fishman and Bazylak [22] used high resolution microscale visualization and measured the through-plane porosity of PTFE-treated GDLs. Studying the GDL through-plane porosity, a higher local porosity in the center of the GDL and a lower local porosity near the surface were observed. This observation was attributed to a higher PTFE concentration near the surface and a lower PTFE concentration in the core region of the GDL. In another study, Rofaiel et al. [42] used scanning electron microscopy (SEM) energy dispersive X-ray to measure the through-plane PTFE distribution within the GDL. They reported a higher PTFE concentration near the surfaces and a lower PTFE concentration in the core region of the GDL. Both studies agree on the heterogeneous through-plane PTFE distribution within the GDL. This uneven profile of the PTFE distribution can be a reason for the different droplet detachment diameters for different PTFE contents. Agglomerated PTFE particles through the GDL increase the internal contact angle θ and decrease the pore radius r_{pore} of the GDL. Such changes result in an increase in the capillary pressure required to intrude liquid water into the pores:

$$P_c = \frac{2\sigma_{water}\cos\theta}{r_{pore}} \quad (4)$$

Liquid water can pass through the pores only when its pressure exceeds the capillary pressure, and for a continuous flow to happen, its pressure should remain higher than the capillary pressure [43].

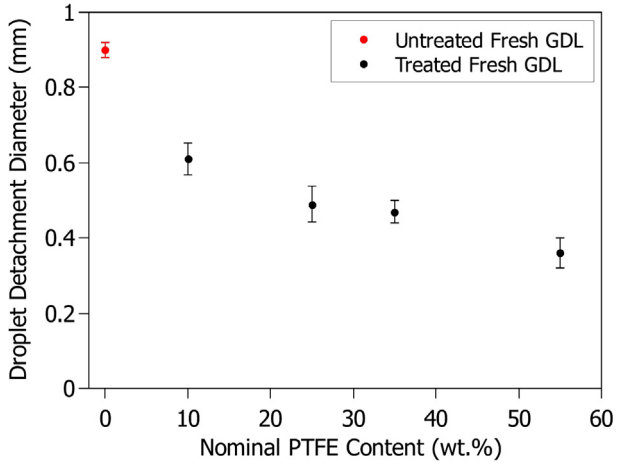

Fig. 9. Droplet detachment diameter under 11.1 m s^{-1} superficial air velocity and at different PTFE wt.% for treated GDL. Sliding diameter is considered for untreated GDL (runs A1–A5 in Table 2).

Carbon layers with high amounts of PTFE content within the GDL resist liquid water transport by acting as a barrier. Low pressure liquid water is not capable of passing through this barrier and accumulates behind the GDL with increasing pressure. The liquid water pressure increases until it reaches the capillary pressure and can pass through the pores. As liquid water passes through the pores, its pressure suddenly drops, and the barrier again blocks water transport through the GDL. The liquid water passing through the GDL appears in the form of droplets on the GDL surface. On the other hand, because the barrier within the GDL has blocked water transport through the GDL, no water column exists underneath the droplet to assist its adhesion [33]. All of these consequences result in easier droplet detachment from the surface of the GDL.

A smaller droplet detachment diameter for GDLs with a higher amount of PTFE may also be justified based on the surface roughness. It has been reported that the droplet behavior on a GDL surface is mostly controlled by the wetting characteristic of the top few monolayers [44]. A higher PTFE concentration has been reported to reduce the surface roughness [22], and because droplets show less of a tendency to detach from rough surfaces [32], it can be concluded that droplets can detach more easily from GDLs with a higher amount of PTFE.

The droplet behavior on untreated GDL surface was also studied in this work. For a treated GDL, droplets could detach from the GDL surface as discussed earlier. However, for an untreated GDL, it was observed that droplets do not detach from the surface. Instead, the emerged droplets were removed by sliding on the GDL surface to the end of the gas channel, where they were discharged through the outlet port. The droplet sliding diameter on an untreated GDL is shown in Fig. 9. Fig. 10 shows a droplet sliding on an untreated GDL without being detached. Fairweather et al. [17] measured the capillary pressure for untreated and treated GDLs and found that liquid water intrudes more easily into an untreated GDL, while adding a slight amount of PTFE to the GDL makes it easier to remove water and harder for the water to intrude.

The effect of GDL aging on the droplet detachment diameter was not studied in this work. However, although aging was observed to decrease the droplet contact angles (Fig. 5), it was assumed that it does not have any effect on the droplet detachment diameter. The reason for this assumption can be explained by the uniform contact angles of droplets on treated aged GDLs. Droplets make similar contact angles on treated aged GDLs with different amounts of PTFE content. Because identical behavior was observed for treated fresh GDLs, it may be assumed that aging has no impact on the droplet detachment diameter.

Our results in this work show that increasing the PTFE content in the GDL enhances droplet detachment by reducing the growth time and the droplet diameter upon detachment. However, the way that the PTFE content affects other parameters should be carefully considered for an appropriate cell design. An optimum PTFE content in the GDL should be defined by considering all of the parameters affecting the cell performance. For instance, in terms of the cell performance, Velayutham et al. [45] reported that the optimum PTFE content is approximately 20 wt.%. Any further amount of PTFE within the GDL increases the electrical resistance, and a lesser amount of PTFE results in water flooding within the cell. Each of these consequences can reduce the cell's performance and should be avoided.

Fig. 11 shows the droplet detachment diameter under a superficial hydrogen velocity of 40 m s^{-1} and as a function of the PTFE content in the GDL. The general trend indicates that the droplet detachment diameter decreases as the PTFE content increases. However, the comparable detachment diameters for 25 wt.% and 35 wt.% suggest that the detachment diameter is not a strong function of the PTFE content within the GDL. A similar observation can be detected in Fig. 9 when air is supplied in the gas channel.

3.3.2. *Effect of the superficial gas velocity on the droplet detachment diameter in the cathode and anode*

The superficial gas velocity plays an important role in droplet detachment from the GDL surface. For a low superficial gas velocity, the drag force applied from the core gas flow (Eq. (3)) cannot overcome the adhesion force. In this case, the droplet increases in size and forms slug. A high superficial gas velocity, on the other hand, leads to low reactant utilization, increased parasitic losses, and possibly membrane dehydration. Therefore, knowing the appropriate range of the superficial gas velocity can lead to an appropriate cell design in terms of liquid water drainage and the overall cell efficiency. Fig. 12 shows the droplet detachment diameter for different superficial air velocities. As the superficial air velocity increases, the droplets detach at smaller diameters on the treated GDL surface. For an untreated GDL, increasing the superficial air velocity decreases the droplet sliding diameter. It was observed that for low superficial air velocities (3.7 m s^{-1} and

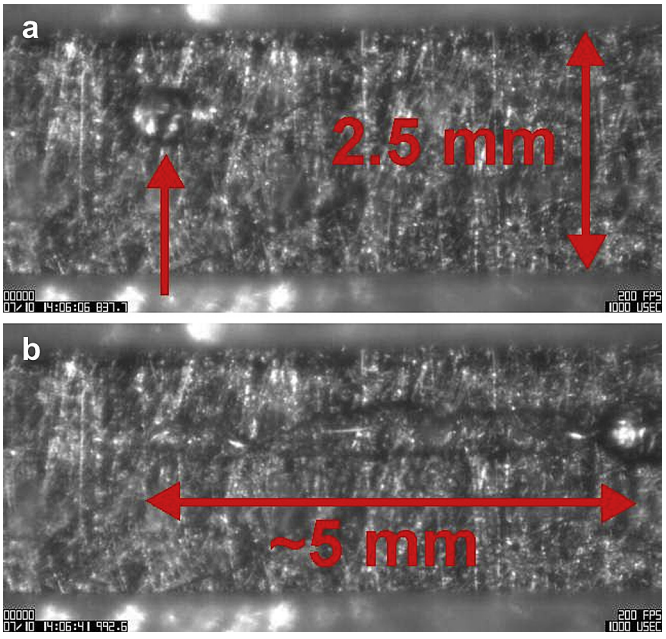

Fig. 10. Droplet sliding on untreated GDL without detaching.

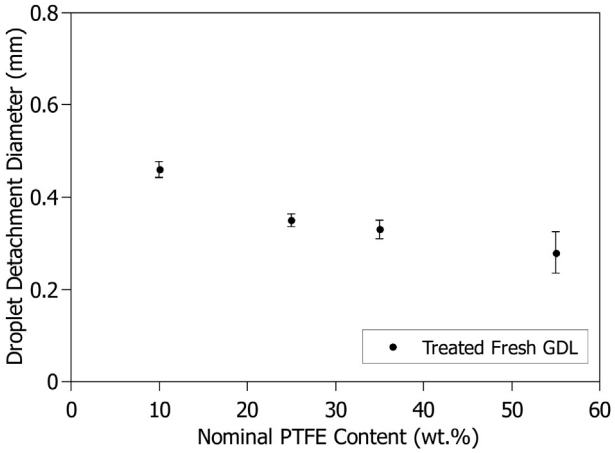

Fig. 11. Droplet detachment diameter under 40 m s^{-1} superficial hydrogen velocity with different PTFE wt.% (runs H1–H4 in Table 2).

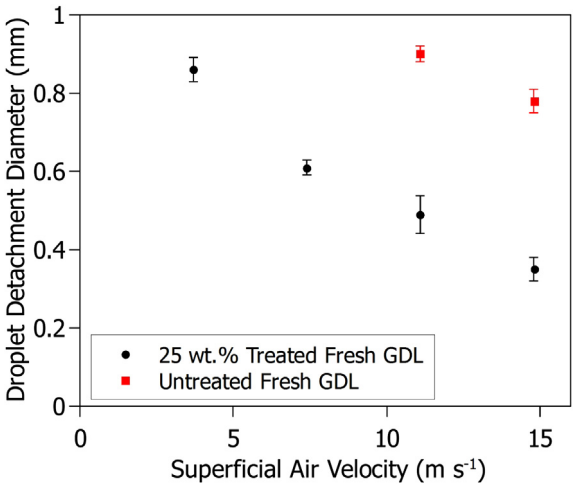

Fig. 12. Droplet detachment diameter under different superficial air velocities and 25 wt.% PTFE treated and untreated GDL (runs A1, A3, A6–A8 and A9).

7.4 m s^{-1}), droplets were not sliding on untreated GDLs. Instead, they grew in size and turned into slugs.

Fig. 13 shows the droplet detachment diameter as a function of the superficial hydrogen velocity. The general trend is that the droplet detachment diameter decreases as the superficial hydrogen velocity increases. The droplet detachment diameter for two different PTFE contents (25 wt.% and 35 wt.%) is plotted in this figure. For a low to moderate superficial hydrogen velocity (20 m s^{-1}–33.3 m s^{-1}), the droplet detachment diameter is lower for 35 wt.%, while for a higher superficial hydrogen velocity (40 m s^{-1}–53.3 m s^{-1}), the droplets detach at comparable diameters from the GDLs. This behavior indicates that for a high superficial gas velocity, the PTFE content in a GDL is not the governing parameter in droplet detachment.

In reality, the hydrogen velocity in the anode tends to be low because pure hydrogen is used and utilization is very high. Therefore, once droplets form in the anode gas channel, it is extremely difficult to remove such droplets by the drag force.

3.3.3. *Comparing the sensitivity of the PTFE content in a GDL and the superficial gas velocity on the droplet detachment diameter*

The droplet growth and detachment from a treated fresh GDL under the influence of a shear gas flow is studied. Although

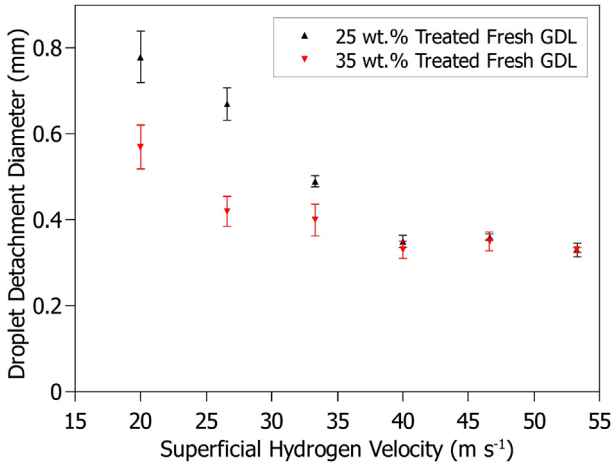

Fig. 13. Droplet detachment diameter for different hydrogen superficial velocity in gas channel (runs H2, H3, H5–H14).

increasing both the PTFE content in the GDL and the superficial gas velocity in the gas channel were observed to decrease the droplet detachment diameter, the latter was found to have more of an impact on the size of the droplet upon detachment. As the superficial air velocity increased from 3.7 m s^{-1} to 14.8 m s^{-1}, the droplet detachment diameter decreased from 0.86 mm to 0.35 mm for a 25 wt.% treated GDL (Fig. 12). However, for a constant superficial air velocity of 11.1 m s^{-1}, increasing the PTFE content within the GDL from 10 wt.% to 55 wt.% resulted in a droplet detachment diameter reduction from 0.61 mm to 0.36 mm (Fig. 9). These results show that between the PTFE content within the GDL and the superficial gas velocity flowing in gas channel, the superficial gas velocity is a sensitive parameter that affects the droplet detachment diameter. The droplet growth and removal from untreated GDL is also investigated. Despite treated GDLs where droplets could detach from the GDL surfaces, the droplet removal from an untreated GDL surface was in the form of droplet sliding. For a high superficial air velocity, the core gas flow was capable of sliding the droplet on the GDL surface, while for a low air flow rate, the droplets increased in size and turned into slugs (Fig. 12).

4. Conclusion

The water droplet emergence, growth, and detachment on GDLs with different PTFE contents are studied under different superficial gas velocities. To simulate droplet behavior in the anode and cathode of an operating PEFC, hydrogen and air were supplied, respectively, within the gas channel. The following conclusions can be drawn from this study:

1. Applying PTFE on a raw GDL increases the contact angle significantly, but the contact angle does not change for different PTFE contents. Furthermore, droplets show much more uniform contact angles on treated GDLs compared to untreated ones. As GDLs are loaded with PTFE, PTFE particles fill the GDL pores and make the GDL surfaces more uniform with shorter contact lines between the droplet and fibers.
2. Droplets show slightly lower contact angles on treated aged GDLs compared to fresh ones. This is an indication of PTFE degradation from the GDL surface. However, because the average contact angle measured on treated fresh GDLs ($\sim 152^\circ$) and treated aged GDLs ($\sim 148^\circ$) are almost similar, it is assumed that GDL aging does not have any effect on the droplet detachment diameter.
3. The droplet detachment diameter decreases as the PTFE content in the GDL increases. A high PTFE content within the GDL increases the capillary pressure liquid water needs to exceed to be able to pass through the GDL pores. The increased liquid water pressure provides the liquid a path through the pores, but as liquid water passes through the GDL, its pressure instantly drops. This results in small droplets emerging from the GDL surface without water columns underneath to assist adhesion. A smaller droplet detachment diameter can also be obtained by a smoother GDL surface. Droplets tend to detach easily from less rough surfaces. As PTFE treating makes GDL surfaces smoother, droplets can be detached from GDLs with a higher amount of PTFE at a smaller diameter.
4. The superficial gas velocity significantly affects the droplet detachment diameter. Increasing the superficial gas velocity increases the drag force applied on the droplet. Therefore, a smaller droplet diameter is required to overcome the adhesion force keeping the droplet on the GDL surface.
5. It was observed that droplets detach at higher superficial velocities for hydrogen than for air. Hydrogen's lower density is the main reason for this effect.

6. It was observed that droplet detachment does not occur on an untreated GDL. Instead, the droplets slide on its surface all the way to the end of the gas channel. This results from the lower contact angle (higher surface energy) of the droplets on untreated GDLs.
7. For a high superficial hydrogen velocity (40 m s^{-1}–53.3 m s^{-1}), the PTFE content in the GDL is not the governing parameter in defining the droplet detachment diameter. Similar detachment diameters were recorded for GDLs with two different amounts of PTFE.

Acknowledgments

Michigan Technological University is gratefully acknowledged for providing the startup fund for this research. The authors would like to thank Vinaykumar Konduru from *Microfluidic and Interfacial Transport Laboratory* [35] at Michigan Technological University for measuring the contact angles of droplets on GDLs. M. Mortazavi also thanks Amir Shahmoradi and Azad Henareh for their fruitful discussions during this research.

References

[1] A. Faghri, Z. Guo, Int. J. Heat Mass Transfer 48 (19) (2005) 3891–3920.
[2] U. Pasaogullari, C.Y. Wang, J. Electrochem. Soc. 151 (2004) A399–A406.
[3] J. Ihonen, M. Mikkola, G. Lindbergh, J. Electrochem. Soc. 151 (8) (2004) A1152–A1161.
[4] I.S. Hussaini, C.Y. Wang, J. Power Sources 187 (2) (2009) 444–451.
[5] F.Y. Zhang, X.G. Yang, C.Y. Wang, J. Electrochem. Soc. 153 (2006) A225.
[6] M. Mathias, J. Roth, J. Fleming, W.L. Lehnert, in: W. Vielstich, A. Lamm, H.A. Gasteiger (Eds.), Handbook of Fuel Cells: Fundamentals, Technology, and Applications, Wiley, Chichester, England/Hoboken, NJ, 2003, p. 121.
[7] V.A. Paganin, E.A. Ticianelli, E.R. Gonzalez, J. Appl. Electrochem. 26 (1996) 297–304.
[8] G.G. Park, Y.J. Sohn, T.H. Yang, Y.G. Yoon, W.Y. Lee, C.S. Kim, J. Power Sources 131 (2004) 182–187.
[9] C. Lim, C.Y. Wang, Electrochim. Acta 49 (24) (2004) 4149–4156.
[10] J. Song, S. Cha, W. Lee, J. Power Sources 94 (1) (2001) 78–84.
[11] G. Lin, T.V. Nguyen, J. Electrochem. Soc. 152 (2005) A1942.
[12] J. Lobato, P. Canizares, M. Rodrigo, C. Ruiz-López, J. Linares, J. Appl. Electrochem. 38 (6) (2008) 793–802.
[13] K. Tüber, D. Pócza, C. Hebling, J. Power Sources 124 (2) (2003) 403–414.
[14] S. Ge, C.Y. Wang, J. Electrochem. Soc. 154 (10) (2007) B998–B1005.
[15] D. Spernjak, A.K. Prasad, S.G. Advani, J. Power Sources 170 (2007) 334–344.
[16] W. Dai, H. Wang, X.Z. Yuan, J. Martin, J. Shen, M. Pan, Z. Luo, J. Power Sources 188 (1) (2009) 122–126.
[17] J.D. Fairweather, P. Cheung, D.T. Schwartz, J. Power Sources 195 (3) (2010) 787–793.
[18] J.T. Gostick, M.A. Ioannidis, M.W. Fowler, M.D. Pritzker, J. Power Sources 194 (1) (2009) 433–444.
[19] D. Bevers, R. Rogers, M.V. Bradke, J. Power Sources 63 (2) (1996) 193–201.
[20] O.S. Burheim, J.G. Pharoah, H. Lampert, P.J. Vie, S. Kjelstrup, J. Fuel Cell Sci. Technol. 8 (2) (2011).
[21] L. Giorgi, E. Antolini, A. Pozio, E. Passalacqua, Electrochim. Acta 43 (24) (1998) 3675–3680.
[22] Z. Fishman, A. Bazylak, J. Electrochem. Soc. 158 (2011) B841.
[23] J.P. Owejan, T.A. Trabold, D.L. Jacobson, M. Arif, S.G. Kandlikar, Int. J. Hydrogen Energy 32 (17) (2007) 4489–4502.
[24] M.A. Hickner, N.P. Siegel, K.S. Chen, D.S. Hussey, D.L. Jacobson, M. Arif, J. Electrochem. Soc. 155 (2008) B427.
[25] M.M. Mench, Q.L. Dong, C.Y. Wang, J. Power Sources 124 (1) (2003) 90–98.
[26] X.G. Yang, N. Burke, C.Y. Wang, K. Tajiri, K. Shinohara, J. Electrochem. Soc. 152 (2005) A759.
[27] P.K. Sinha, P. Halleck, C.Y. Wang, Electrochem. Solid-State Lett. 9 (7) (2006) A344–A348.
[28] S.J. Lee, N.Y. Lim, S. Kim, G.G. Park, C.S. Kim, J. Power Sources 185 (2) (2008) 867–870.
[29] E.C. Kumbur, K.V. Sharp, M.M. Mench, J. Power Sources 161 (1) (2006) 333–345.
[30] X.G. Yang, F.Y. Zhang, A.L. Lubawy, C.Y. Wang, Electrochem. Solid-State Lett. 7 (2004) A408.
[31] A. Theodorakakos, T. Ous, M. Gavaises, J.M. Nouri, N. Nikolopoulos, H. Yanagihara, J. Colloid Interf. Sci. 300 (2) (2006) 673–687.
[32] A. Bazylak, D. Sinton, N. Djilali, J. Power Sources 176 (1) (2008) 240–246.
[33] P.K. Das, A. Grippin, A. Kwong, A. Weber, J. Electrochem. Soc. 159 (2012) 489–496.
[34] C.M. Hwang, M. Ishida, H. Ito, T. Maeda, A. Nakano, Y. Hasegawa, N. Yokoi, A. Kato, T. Yoshida, Int. J. Hydrogen Energy 36 (2010) 1740.
[35] http://www.me.mtu.edu/mnit/.
[36] V. Konduru, Master's thesis, Michigan Technological University, 2010.
[37] T.C. Wu, N. Djilali, J. Power Sources 208 (2012) 248–256.
[38] C.N. Lam, N. Kim, D. Hui, D.Y. Kwok, M.L. Hair, A.W. Neumann, Colloid Surf. A 189 (1) (2001) 265–278.
[39] J. Benziger, J. Nehlsen, D. Blackwell, T. Brennan, J. Itescu, J. Membr. Sci. 261 (1–2) (2005) 98–106.
[40] A. Bazylak, D. Sinton, Z.S. Liu, N. Djilali, J. Power Sources 163 (2) (2007) 784–792.
[41] J. Allen, J. Colloid Interf. Sci. 261 (2) (2003) 481–489.
[42] A. Rofaiel, J.S. Ellis, P.R. Challa, A. Bazylak, J. Power Sources 201 (2012) 219–225.
[43] J.H. Nam, M. Kaviany, Int. J. Heat Mass Transfer 46 (24) (2003) 4595–4611.
[44] G.M. Whitesides, P.E. Laibinis, Langmuir 6 (1) (1990) 87–96.
[45] G. Velayutham, J. Kaushik, N. Rajalakshmi, K.S. Dhathathreyan, Fuel Cells 7 (4) (2007) 314–318.